ZIBELINE INTERNATIONAL™ PUBLISHING

Water Conservation & Management (WCM)

DOI: http://doi.org/10.26480/wcm.01.2022.45.50

ISSN: 2523-5664 (Print)
ISSN: 2523-5672 (Online)
CODEN: WCMABD

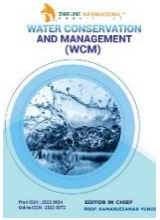

RESEARCH ARTICLE

OPTIMISATION OF ACTIVATED CARBON PRODUCTION FROM BAOBAB FRUIT SHELLS BY CHEMICAL ACTIVATION WITH KOH FOR THE REMOVAL OF PHENOL

Radhia Nedjai, Nassereldeen Ahmed Kabbashi*, Md Zahangir Alam, Ma'an Fahmi Rashid Alkhatib

Department of Biotechnology Engineering, Kulliyyah of Engineering, International Islamic University, Malaysia.
Corresponding Author Email: nasreldin@iium.edu.my

ARTICLE DETAILS

Article History:

Received 15 December 2021
Accepted 27 January 2022
Available online 04 February 2022

ABSTRACT

Activated carbons (ACs) were produced from baobab fruit shell (BFS) by varying the operating parameters of activation temperatures, activation times, and impregnation ratios using response surface methodology (RSM). Adsorption tests on an aqueous solution of phenol were used to determine the optimum conditions for BF-ACs produced and central composite design (CCD) was used to determine the effects of the three preparation variables on the adsorption capacity of phenol. Based on the CCD, a quadratic equation was developed for the response, and from the analysis of variance (ANOVA), the most significant factor was specified. The results demonstrated that the optimal activated carbon which had the highest phenol adsorption capacity (93.56 mg/g) was obtained by these conditions as follows: the activation temperature of 700 °C, the activation time of 60 min, and IR of 2. Characterisation of the BF-AC produced showed that good quality adsorbents with the few functional groups and the distribution of the well-forming pores are found during the optimum production conditions. The highest BET surface area and micropore volume were 1263.127 m^2/g and 0.453 cm^3/g, respectively. It concluded that activated carbons produced from baobab fruit shells using KOH are suitable for the treatment of wastewaters from organic pollutants.

KEYWORDS

Activated Carbon, Baobab Fruit Shells, Optimisation, Phenol Adsorption, Response surface methodology.

1. INTRODUCTION

Industrial processes generate a variety of molecules that can pollute the air and the water because of their harmful impacts (toxicity, carcinogenic and mutagenic properties) on habitats and people. Phenol is one of the most important organic water contaminants, as it is harmful even at low concentrations (Busca et al., 2008). Owing to insufficient treatment by such industrial effluents of these hazardous compounds, soils, groundwater, and water sources are extensively polluted and their toxicity seriously affects living microorganisms (Alam et al., 2007). They generate an oxygen demand in receiving waters and affect the odour and taste of drinking water at even small, chlorinated derivatives concentrations. Water treatment plants usually disinfect water using chlorination, therefore, the undesirable chlorophenols formed in the presence of phenols (Alam et al., 2007).

The phenolic compounds were found to be persistent bio-accumulative and toxic (PBT) chemicals, which linger for prolonged periods in the environment, even in minute quantities, that affect many organisms' generations (Abd-Hadi and Salman, 2020; Check and Marteel-Parrish, 2013). Considering the toxicity of phenol, the U.S. Environmental Protection Agency (USEPA) has listed phenols as a priority pollutant, with a permissible limit of 0.1 mg/L in wastewater and 0.001 mg/mL in water supplies (Abd-Hadi and Salman, 2020; Xie et al., 2020). In the aquatic environment, phenol greatly reduces the consumption of fish food, mean weight, and fertility, thus, their toxicity level for fish has been estimated to range between 9-25 mg/L (Gad and Saad, 2008). Whereas the level of phenol toxicity of human beings ranges from 10 to 24 mg/L and its lethal concentration in the blood is 150 mg/ 100 mL, and the excessive exposure or inhalation of these compounds may cause coma, vomiting, cyanosis, and other adverse events (Sunil and Jayant, 2013; Ahmaruzzaman, 2008; Busca et al., 2008).

Numerous conventional techniques for phenol removal from wastewater are reported including chemical oxidation, coagulation, biodegradation, ion exchange, chemical precipitation, membrane filtration, immobilization, and reverse osmosis (Al-Obaidi et al., 2018; Jiang et al., 2015; Ogando et al., 2019; Sharma and Philip, 2014; Ochando-Pulido et al., 2018; Sridhar et al., 2018; Zagklis et al., 2015; Víctor-Ortega et al., 2016). However, these techniques are generally identified with certain drawbacks such as high cost, generate more dangerous products, and high energy intensity (Abd-Hadi and Salman, 2020). Various research have revealed that adsorption is the most effective technique for removing the traces of these organic compounds from wastewater (Rashed, 2013). The activated carbon is the most commonly utilised adsorbent owing to its excellent organic adsorption ability (Xie et al., 2020).

Activated Carbon is a versatile adsorbent, which has been used since ancient times by Egyptians and Indians (Kundu et al., 2015). It has a high porosity and a large specific surface area. In modern times, activated carbon has been widely utilized by the chemical industry for purifying, dechlorinate, decolorize, separating, and concentrate to enable recovery and filtration (Bansal and Goyal, 2005). Furthermore, it has been used to remove the unfavourable constituents from gases and liquid solutions. Therefore, it is utilized in a variety of domains, such as pharmaceutical, chemical, nuclear, naphtha, and for the drinking water treatment and wastewater (Kundu et al., 2015). Commercially available activated carbon is an excellent absorbent, but it is expensive, as its market price usually

Quick Response Code	Access this article online	
	Website: www.watconman.org	**DOI:** 10.26480/wcm.01.2022.45.50

Cite the Article: Radhia Nedjai, Nassereldeen Ahmed Kabbashi, Md Zahangir Alam, Ma'an Fahmi Rashid Alkhatib (2022). Optimisation of Activated Carbon Production From Baobab Fruit Shells by Chemical Activation With Koh for the Removal of Phenol. *Water Conservation & Management, 6(1): 45-50.*

ranges from about $ 1,000 to $ 3,000 per ton (Sudibandriyo and Kusumadewi, 2018). This is a major water treatment difficulty.

Therefore, appears necessary to use new and alternative sources, which should be efficient, low cost, and available for activated carbon production. It was found that the use of agricultural residue as precursors is comparatively cheaper and effective (Yahya et al., 2015). Moreover, they are non-toxic, available in large quantities, renewable, and easily accessible sources. In general, activated carbon precursors are agricultural residues with lignocellulose and carbon content (Sudibandriyo and Kusumadewi, 2018). Baobab fruit shell (BFS) is one of the potential activated carbon precursors owing to its abundance and cheap cost. According to a previous study, the baobab fruit shell consists of 54.08% lignin, 24.87% of cellulose, 21.05% of hemicellulose content, ash content 5.17%, moisture content 6.48%, 86.73% of volatile matter, and 1.22% carbon content .

As the performance of activated carbon is significantly affected by various factors during the synthesis process, thus, it is essential to determine the optimum conditions in the production process of activated carbon. The use of the response surface methodology (RSM) to analyse the impact of process variables on the targeted response in chemical processes could accomplish this goal. In addition to accurate statistical data on the process, RSM permits the usage of experimental design with a minimum number of runs that save time, materials, and hence cost (Md Arshad et al., 2019).

Many experiments have been carried out on the experiment design and data processing using RSM. There is however still a lack of literature on optimisation in the development of baobab fruit shell for phenol adsorption. Therefore, this study was aimed to demonstrate the production of activated carbons based on baobab fruit shell (BFS) and their adsorptive capacities on phenol removal. Several reaction parameters were investigated to evaluate the performance of activated carbons produced in an aqueous solution of phenol using RSM designs, which included activation temperatures, time activations, and impregnation ratio (IR). The surface functional groups, textural properties, and BET surface area of the BF-ACs were also investigated.

2. Materials and Methods

2.1 Materials

Potassium hydroxide (KOH) used as an activating agent for the activation process that was purchased from R&M Chemicals. Baobab fruit shells (BFS) were obtained from West Sudan that were utilized as raw material to produce the activated carbon. Nitrogen gas (99.95%) was acquired from Fuelink Marketing Sdn, Bhd. that was utilized for inert atmosphere over the carbonization process. Phenol of reagent grade was acquired Sigma-Aldrich.

2.2 Production of BF-ACs

Baobab fruit shells (BFS) were acquired from West Sudan that was used as the precursor to produce the activated carbon. The baobab fruits were opened to isolate the seeds from the shells. Then, the shells were reduced by scissors in sizes from 1 to 2 cm and were washed serval time with tap water and finally with distilled water to remove any impurities. The samples were dried in the oven at 105 °C until a constant weight was obtained. The resulting samples were milled and were sieved to obtain a fraction of the size of 1 mm. The samples were mixed with KOH using different impregnation ratios (IR) (raw material: KOH (w:w)). A volume of distilled water equals to 4 times the all-out mass of the mixture was added. The mixture was agitated for 60 min at 50 °C in the rotary shaker and was placed to the oven overnight at 100 °C. A few minutes before staring carbonization, the quartz tube was purged with high-purity nitrogen gas (N_2) at a rate of 0.3 L/m, which was preserved during the activation and cooling stages. The carbonization of BFS samples was carried out in a Lenton horizontal tubular quartz reactor (England, UK) and a Carbolite horizontal tube electrical furnace (Model CTF, UK) at different conditions defined by the experimental design (DoE). The activated product was taken out from the quartz tube and moved to a desiccator for cooling, then neutralized with 50 mL of HCl (0.5 M) solution and washed with warm distilled water until a constant pH of the washing solution was achieved. The activated carbon was dried in the oven at 110 °C.

2.3 Design of experiments

According to literature, activation temperature, impregnation ratio, and activation time are defined as the most significant factors in the activation (carbonization) of KOH based activated carbon (Abdel-Ghani et al., 2016; Mamaní et al., 2019; Niasar et al., 2018). Therefore, the optimal conditions for activated carbon preparation from BFS were determined by examining the effects of these three parameters using Face-cantered Central Composite Design (FCCCD), which was selected for a minimum number of experiments to fit a quadratic surface for the response. The FCCCD consists of three types of runs which are the 2^n factorial runs, 2(n) axial runs, and 6 centre runs, where n is the number of variables. A total of 20 experiments were obtained by a statistical software of the Design of experiment (DoE) for this procedure as calculated using Eq. (1).

$$N = 2 \ + 2n + n_c = 2^3 + 2^*3 + 6 = 20 \quad (1)$$

where N is the total experiments needed number.

Based on the literature and preliminary studies, the range of these variables has chosen, which are reported in Table 1.

Table 1: Experimental factors and their high and low level for central composite design (CCD)

Factor	Name	Low level (-)	High level (+)
A	Activation temperature	500	900
B	Activation time	30	90
C	Impregnation ratio	1:1.5	1:2.5

2.4 Batch Adsorption Experiments

To evaluate the adsorption capacity of the prepared BF-ACs toward the phenol, a series of 100 mL-conical flasks contain 0.025 g of dried activated carbon and 25 mL aqueous solution of phenol at pH 6 with a concentration of 100 mg/L was stirred at room temperature (27±1°C) using a rotary shaker at 200 rpm. The Uvi light spectrophotometer (UviLine 9400, Secomam, France) was used to determine the residual concentration of phenol at 270 nm. The standard calibration curve used to determine the final phenol concentration. The amount of phenol adsorbed was determined as the follows:

$$q_e = \frac{(C_i - C_f)V}{W} \quad (2)$$

where the quantity of phenol adsorbed per gram of biosorbent at equilibrium (mg/g) represented by (q_e), the initial phenol concentration represented by C_i (mg/L), the final or equilibrium phenol concentration represented by C_f (mg/L), the volume of phenol solution in the flasks represented by V (L) and the weight of biosorbent used represented by W (g) (Nedjai et al., 2021). The difference between phenol concentration before and after adsorption (C_i–C_f) to the initial concentration of phenol in the aqueous solution (C_i) is knowing as the percentage of phenol removal, and it may be estimated as follows:

$$Removal\ Percentage = \frac{(C_i - C_f)}{C_i} \times 100 \quad (3)$$

2.5 Statistical Analysis

The data obtained from experimental runs were studies and interpreted using the statistical software Design-Expert version 12.0.12.0 (STAT-EASE, Inc., Minneapolis, US) for the regression analysis in accordance with the second-degree polynomial equation and to determine the statistical value of the formed equations.

2.6 Characterisation of BF-ACs

2.6.1 BET surface area

Physical adsorption of N_2 (at 77 k) was utilized to characterise the porosity of the BF-ACs using Quantachrome, Autosorb-1C and a surface area analyzer according to the Brunauer–Emmett–Teller (BET) model. Preceding the measurement, the BF-ACs outgassed at 300°C for 4 hrs using a vacuum. The data have been subjected to certain mathematical analysis to determine a surface area.

2.6.2 The XRD

X-ray Diffraction (XRD) analysis were performed utilizing Bruker D2 Phaser (Bruker AXS, Karlsruhe, Germany) diffractometer equipped with a copper anode (Cu Kα = 1.54184 Å) throughout a scanning interval (2θ) between 20 and 80 degrees at a scan speed of 0.25 s/step.

2.6.3 Fourier Transform Infrared (FT-IR)

Fourier transform infrared (FT-IR) spectroscopic was applied to analysis the surface chemistry of raw baobab fruit shell and activated carbon

prepared using a Perkin Elmer Frontier model FTIR-spectrometer. Thermo Scientific Nicolet™ model iS50 FTIR Spectrometer was used to record the wavelengths spectrums of the specimens between 4000 and 400 cm^{-1}.

3. Results and Discussion

3.1 Optimisation of physical conditions for BF-ACs

Statistical analysis of the data collected for phenol adsorption of the 20 different samples, prepared according to the design matrix, was analysed with the Design of Expert software. The different parameters which were optimised using FCCCD are activation temperature, activation time, and the impregnation ratio. The response was phenol adsorption capacity. The complete design matrixes and the response values are presented in Table 2. The maximum adsorption capacity (q_e) of BF-ACs were found to range from 75.08 to 93.56 mg/g. The highest adsorption capacity of 93.56 mg/g was found at 700 °C, activation time of 60 min, and 1:2 impregnation ratio. In order to determine the optimum activation conditions of BF-AC for the enhancement of adsorption capacity (mg/g), the regression model was developed. The model has the following equation:

$$Adsorption\ Capacity = -35.36118 + 0.16277\,A + 0.369611\,B + 50.33157\,C - 0.000073\,AB - 0.001813\,AC + 0.137083\,BC - 0.000103\,A^2 - 0.004057\,B^2 - 13.68545\,C^2 \quad (4)$$

where A, B and C are the activation temperature (°C), the activation time (min), and the impregnation ratio, respectively.

Table 2: The adsorption capacity results of BF-ACs produced for its optimum production.

Run	Variables			Response
	A: Temperature (°C)	B: Time (min)	C: Impregnation Ratio	Adsorption Capacity, q_t (mg/g)
1	700	60	2	92.17
2	500	60	2	86.66
3	900	90	2.5	90.36
4	700	60	2	91.37
5	500	90	2.5	85.08
6	700	60	2	92.96
7	500	30	1.5	75.08
8	700	60	2	93.56
9	700	60	2	92.56
10	700	90	2	91.71
11	900	30	2.5	78.65
12	900	90	1.5	82.23
13	700	60	1.5	87.2
14	700	60	2	92.56
15	700	30	2	85.61
16	900	30	1.5	82.83
17	500	90	1.5	80.31
18	900	60	2	89.78
19	700	60	2.5	90.58
20	500	30	2.5	75.71

The suitability of the models is justified by the variance analysis (ANOVA) for the adsorption capacity of phenol by produced activated carbon. As shown in Table 3, the quadratic model to be highly significant for assessing the phenol removal, where the *F*-value was 59.05. There was only a 0.1% probability that the "Model *F*-value" this large might occur owing to noise. The *p*-values were less than 0.0500 indicating the model terms are significant. The results also showed that the activation temperature (A), activation time (B), and the impregnation ratio (C) were highly significant since their *p*-values were <0.0001, 0.0001, and 0.0047, respectively. Consequently, these factors had a great effect on the adsorption properties of the baobab fruit shell-based activated carbon produced. The "Lack of Fit *F*-value" of 3.54 implies the Lack of Fit is not significant relative to the pure error. There was a 9.56 % chance that a "Lack of Fit *F*-value" this large might occur owing to noise. A non-significant lack of fit is good as it shows that the model is in a good fit. A non-significant lack of fit is good because it indicates that the model is fit.

Table 3: Analysis of variance (ANOVA) for the adsorption capacity using BF-ACs

ANOVA for Quadratic model						
Source	**Sum of squares**	**DF**	**Mean of squares**	***F*-Values**	***p*-values**	**Status**
Model	6.57	9	0.7304	59.05	< 0.0001	significant
A-A Temperature	0.4439	1	0.4439	35.89	0.0001	
B-B Time	1.01	1	1.01	81.80	< 0.0001	
C-C Ratio	0.1621	1	0.1621	13.10	0.0047	
AB	0.0152	1	0.0152	1.23	0.2932	
AC	0.0026	1	0.0026	0.2125	0.6547	
BC	0.3383	1	0.3383	27.34	0.0004	
A^2	0.4671	1	0.4671	37.76	0.0001	
B^2	0.3666	1	0.3666	29.64	0.0003	
C^2	0.3219	1	0.3219	26.02	0.0005	
Residual	0.1237	10	0.0124			
Lack of Fit	0.0965	5	0.0193	3.54	0.0956	not significant
Pure Error	0.0272	5	0.0054			
Cor Total	6.70	19				
R-Squared	0.9815					
Adj R-Squared	0.9649					
Pred R-Squared	0.8693					
Adeq Precision	22.2778					
Std. Div.	0.1112					

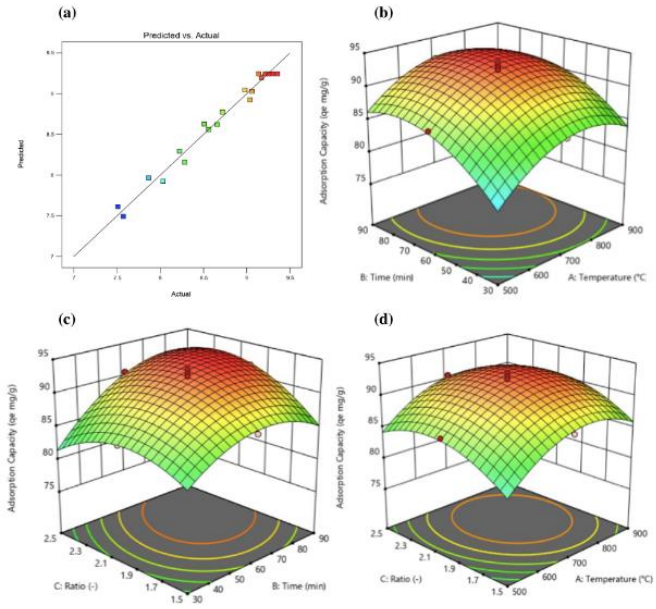

Figure 1: (a) Theoretical vs. experimental values of BF-ACs produced adsorption capacity in aqueous solution of phenol and (b) the 3D plot of the interaction between activation temperature and activation time, (c) activation time and impregnation ratio, and (d) activation temperature and impregnation ratio

The predicted versus actual plot was constructed to compare the experimental values with theoretical values for the adsorption capacity of activated carbon prepared, as shown in Fig. 1a. The theory values obtained are similar to the experimental values, which suggests that the model built has succeeded in bridging the association between activated carbon preparation variables and the adsorption capacity (q_e). The consistency of the developed model was measured on the basis of the

determination value coefficient. The values of the experimental response are correlated to the theoretical response values. The coefficient of determination R^2 of 0.9815 showed that the independent variables – the temperature activation, the activation time, and the impregnation ratio – can explain 98.15 % of the variations of adsorption capacity. The proposed model has also shown that R^2 is in reasonable agreement with the adjusted R^2 values of 0.9649.

3.2 Effect of different factors on the phenol removal

Model equation generated by Design Expert 12.0.12.0 software can be represented graphically and examine the effects of activated carbon preparation factors on adsorption capacity. Figure 1 (b,c,d) represents the 3D response surface plots which were created by plotting the response (adsorption capacity of phenol removal) on the Z-axis against any two independent variables. In the 3D plot presented in Figure 1b, the interactions between activation temperature and activation time are shown. At the lower value, for example 500°C and 30 min, respectively, the adsorption capacity of prepared BF-AC was the lowest (75.08 mg/g).

An increase in the activation temperature and time led to the better quality of AC in terms of its adsorption capacity. Increased activation temperature and time resulted in better BF-ACs adsorption capacity. At 700 °C of activation temperature and 60 minutes of activation time, the adsorption capacity of the BF-AC was about 93.56 mg/g. However, the adsorption capacity of the produced BF-AC decreased again after this stage. In the lower stages, the adsorption trend can be attributed to the partial conversion of the impregnated BFS to activated carbon owing to inadequate activation temperature and activation time. When the activation temperature and time were at the upper end, the interaction resulted in the destruction of the pores structure and carbon burning owing to excessive energy and over exposure, therefore, the lack of adsorption sites did difficult the absorption of the BF-AC (Kundu et al., 2015). Another explanation could be that negatively charged surface groups are decomposed with more material released at high temperatures by KOH activation, particularly the OH group, leading to the decrease of adsorption capacity of the activated carbon (Mopoung et al., 2015).

Figure 1c shows that the adsorption capacity was increasing with the increase of the impregnation ratio and heating time. It was the highest when the impregnation ratio was 1:2 and the activation time was 60 min. At lower levels of IR, the quantities of KOH were too small to react properly with the amounts of the powder baobab fruit shells, so it was not eased to develop micropores and mesopores. With increased impregnation ratios, the more volatile matter is released and more carbon burn-off takes place lead to more mesopores and macropores (Chen et al., 2011). The excess KOH at the high IR might fracture the lignocellulose structure of the baobab fruit shell. Thus, it could not form pores (Kundu et al., 2015). Another explanation might be a high covering with potassium compounds of an activated carbon surface that inhibits the physical surface (Mopoung et al., 2015). Consequently, the adsorption capacity of the BF-AC was difficult.

It was also observed that the adsorption capacity of BF-AC increased, with the increase of the activation temperature and IR in Figure 1d. At 700°C of activation temperature and 1:2 of impregnation ratio, the adsorption capacity of the BF-AC was the highest. Whereas, after this stage, the adsorption capacity of BF-AC decreased, likely because of the burn-out and fracturing of the structure of the raw material, as activation temperatures and IRs increased. The highest phenol adsorption corresponds to the medium of all three variables covered in this study. Similar trend was reported in preparation of porous carbon from coconut shell (Habeeb, 2014).

3.3 Adsorbent characterisation

3.3.1.1 BET Surface Area

The nitrogen adsorption–desorption isotherms of prepared two selected BF-AC samples by the optimisation process (Run 8 and Run 20) presented in Figure 2. The two adsorption isotherms are classified into Type IV isotherm (Figure 2a) and Type I isotherm (Figure 2b), which is described for mesoporous (containing pores 2-50 nm) and adsorbents microporous (containing pores<2nm), as per the IUPAC classification approach (Sotomayor et al., 2018). These findings were compatible with the pore size distribution curve and demonstrated the microporosity of BF-AC_8 (Run 8) and mesoporosity of BF-AC_{20} (Run 20) as shown in Table 4. According to IUPAC classification approach of Hysteresis Loops, the hysteresis loop of BF-AC (Run 20) sample exhibited the Type H1, which is associated with narrow uniform mesopores (Sotomayor et al., 2018).

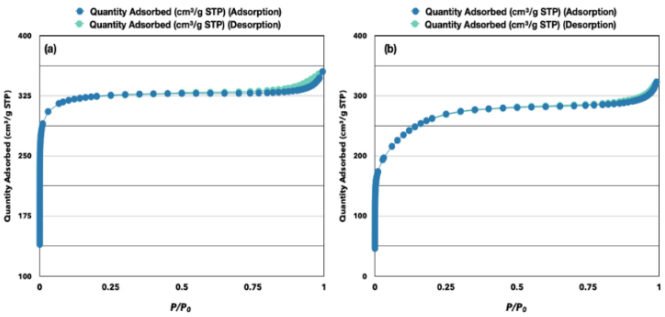

Figure 2: Nitrogen Adsorption–Desorption Isotherms of BF-ACs Samples: (a) Run 20 and (b) Run 8

Table 4 presented BET surface area, pore diameter size, and pore volume of two BF-ACs samples that provided the best phenol adsorption capacity (Run 8) and the bad adsorption capacity (Run 20). According to the results, BF-AC_8 presented higher surface areas of 1263.127 m^2/g compared to BF-AC_{20} of 905.483 m^2/g. It can be seen that the BF-AC_8 is a highly developed specific micropore area of 1151.886 m^2/g, micropore volume of 0.453 cm^3/g, a smaller external surface area of 111.240 m^2/g, and a smaller pore diameter of 1.739 nm in comparison with KOH-AC_{20} sample.

Table 4: BET Surface Area, Pore Diameter sizes, and Pore Volume of BF-ACs (Run 8 and Run 20)

Sample	S_{BET}[a] (m^2/g)	S_{Micro}[b] (m^2/g)	$S_{External}$[c] (m^2/g)	D_{pores}[d] (nm)	V_t[e] (cm^3/g)	V_{Micro}[f] (cm^3/g)
BF-AC_8	1263.127	1151.886	111.240	1.739	0.549	0.4531
BF-AC_{20}	905.483	326.129	579.353	2.207	0.499	0.1511

[a] BET specific surface area, [b] t-Plot Micropore Area, [c] t-Plot External Surface Area, [d] Adsorption average pore diameter, [e] Single point adsorption total pore volume of pores, [f] t-Plot micropore volume

3.3.1.2 X-ray diffraction (XRD)

The X-ray diffraction (XRD) technology is a significant method for analysing materials' crystalline composition. XRD profiles of raw BFS and the selected activated carbon with the highest adsorption capacity were given in Figure 3a. From XRD spectra of the raw BFS and the activated carbon, two Bragg diffraction peaks around 2θ = 20–25° regions and 2θ = 20–30°, respectively. There was no well-defined peak for any aspect of the diffraction profile suggesting that the BFS and AC were not subject to whichever mineral peaks. Other studies have produced similar results and conclusions (Vunain and Biswick, 2018).

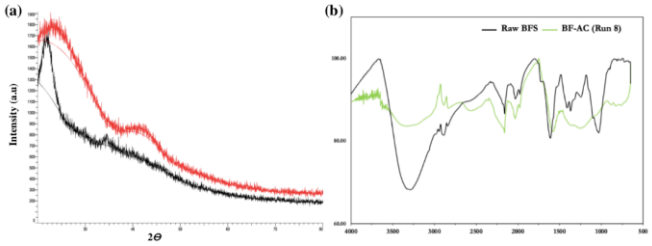

Figure 3: (a) X-ray diffraction patterns of raw BFS and BF-AC (Run 8), (b) FTIR spectra of BFS and the BF-AC (Run 8)

3.3.1.3 FT-IR analysis

The FT-IR spectra for raw BFS and the selected BF-AC were shown in Figure 3b. Generally, it can be seen that the spectrum of raw BFS displays more absorption peaks than the BF-AC spectrum. When some peaks in the raw material disappeared at high-temperature (700 °C) following activation owing to the removal of volatile and heat sensitive functional groups. The presence of a hydrogen-bonded (O – H) group of cellulose and Pectin and Lignin for raw material (BFS) was ascribed to the broadband at 3285,18 cm^{-1} (Vunain and Biswick, 2018). A symmetrical stretching (C – H), and alkyl group (– CH_2), was the product of a bond that was approximately 2889.65 cm^{-1}. Due to the presence of (C≡N) extending, weak peaks at about 2160 cm^{-1} and 2031 cm^{-1} were observed. The peak at 1613.83 cm^{-1} is the aromatic ring or the olefinic (C=C) stretching vibration owing to carboxyl, lactone, ketones, and aldehyde (Vunain et al., 2017).

The presence of (C – O – C) or (C=C) detention, which can be due to the nature of ester, ether and phenol, contributed to a relatively low-intensity band at around 1377 cm^{-1}. The band at 1033.37 cm^{-1} is anhydrides (C-O) characteristics, which disappeared in the activated carbon. Hydroxyl groups, carbonyl groups and carboxyl groups are the main functional groups in raw BFS. On the other hand, activated carbon spectrum present bands at around 2886cm^{-1}, 2161cm^{-1}, 1575cm^{-1}, 1255cm^{-1} were the characteristics of C–H (alkyls), C≡C (alkyne), C–O–C (ester, ether and phenol) and C–O (anhydrides), respectively. Some functional groups, including O-H / N-H, C-O and C = O groups, were disappearing after carbonization, which revealed that a loss of water and hydroxyls occurred during the carbonization.

4. Conclusions

From this study, it was found that the best quality BF-AC with higher phenol adsorption capacity is subjected to activation temperature, heating time, and Impregnation ratio. The suggested optimum operating conditions by the DoE model were 700°C of activation temperature, 60 min of heating time, and 1:2 of impregnation ratio. The experimental adsorption capacity of BF-AC was found to be 93.56 mg/g and the highest BET surface area was reached 1263.127 m^2/g. Characterisation studies revealed that the BF-AC had highly pored surfaces, and FTIR data indicated that the hydrogen component of the raw material was dehydrated and extracted to produce AC. Based on these results of this study, it can be concluded that the baobab fruit shell can be used as a precursor to produce a high surface area and highly effective activated carbon in order to treat polluted waters from organic pollutants.

Acknowledgement

The authors are grateful to the Department of Biotechnology Engineering, Faculty of Engineering, International Islamic University Malaysia for providing continuous support to the research at hand.

References

Abdel-Ghani, N.T., El-Chaghaby, G.A., Elgammal, M.H., Rawash, E.S.A., 2016. Optimizing the preparation conditions of activated carbons from olive cake using KOH activation. Xinxing Tan Cailiao/New Carbon Materials, 31 (5), Pp. 492–500. https://doi.org/10.1016/S1872-5805(16)60027-6

Abd-Hadi, G.M., Salman, S.D., 2020. Adsorption of para nitro-phenol by activated carbon produced from alhagi. Sains Malaysiana, 49 (1), Pp. 57–67. https://doi.org/10.17576/jsm-2020-4901-07

Ahmaruzzaman, M., 2008. Adsorption of phenolic compounds on low-cost adsorbents: A review. Advances in Colloid and Interface Science, 143 (1–2), Pp. 48–67. https://doi.org/10.1016/j.cis.2008.07.002

Alam, M.Z., Muyibi, S.A., Mansor, M.F., Wahid, R., 2007. Activated carbons derived from oil palm empty-fruit bunches: Application to environmental problems. Journal of Environmental Sciences, 19 (1), Pp. 103–108. https://doi.org/10.1016/S1001-0742(07)60017-5

Alam, M.Z., Muyibi, S.A., Toramae, J., 2007. Statistical optimization of adsorption processes for removal of 2,4-dichlorophenol by activated carbon derived from oil palm empty fruit bunches. Journal of Environmental Sciences, 19 (6), Pp. 674–677. https://doi.org/10.1016/S1001-0742(07)60113-2

Al-Obaidi, M.A., Jarullah, A.T., Kara-Zaïtri, C., Mujtaba, I.M., 2018. Simulation of hybrid trickle bed reactor–reverse osmosis process for the removal of phenol from wastewater. Computers and Chemical Engineering, 113, Pp. 264–273. https://doi.org/10.1016/j.compchemeng.2018.03.016

Bansal, R.C., Goyal, M., 2005. Activated Carbon Adsorption.

Busca, G., Berardinelli, S., Resini, C., Arrighi, L., 2008. Technologies for the removal of phenol from fluid streams: A short review of recent developments. Journal of Hazardous Materials, 160 (2–3), Pp. 265–288. https://doi.org/10.1016/j.jhazmat.2008.03.045

Check, L., Marteel-Parrish, A., 2013. The fate and behavior of persistent, bioaccumulative, and toxic (PBT) chemicals: Examining lead (Pb) as a PBT metal. Reviews on Environmental Health, 28 (2–3), Pp. 85–96. https://doi.org/10.1515/reveh-2013-0005

Chen, Y., Huang, B., Huang, M., Cai, B., 2011. On the preparation and characterization of activated carbon from mangosteen shell. Journal of the Taiwan Institute of Chemical Engineers, 42 (5), Pp. 837–842. https://doi.org/10.1016/j.jtice.2011.01.007

Gad, N.S., Saad, A.S., 2008. Effect of Environmental Pollution by Phenol on Some Physiological Parameters of Oreochromis niloticus. Global Veterinaria, 2 (6), Pp. 312–319. https://doi.org/10.1.1.619.7089

Habeeb, O.A., 2014. Optimization and Characterization Study of Preparation Factors of Activated Carbon Derived from Coconut shell to Remove of H2S from Wastewater. In Activated carbon: prepared from various precursors, pp. 44–61.

Jiang, J., Gao, Y., Pang, S.Y., Lu, X.T., Zhou, Y., Ma, J., Wang, Q., 2015. Understanding the role of manganese dioxide in the oxidation of phenolic compounds by aqueous permanganate. Environmental Science and Technology, 49 (1), Pp. 520–528. https://doi.org/10.1021/es504796h

Kabbashi, N.A., Mirghani, M.E.S., Alam, M.Z., Qudsieh, S.Y., Bello, I.A., 2017. Characterization of the Baobab fruit shells as adsorption material. International Food Research Journal, 24, Pp. 472–474.

Kundu, A., Gupta, B.S., Hashim, M.A., Sahu, J.N., Mujawar, M., Redzwan, G., 2015. Optimisation of the process variables in production of activated carbon by microwave heating. RSC Advances, 5 (45), Pp. 35899–35908. https://doi.org/10.1039/c4ra16900j

Mamaní, A., Sardella, M.F., Giménez, M., Deiana, C., 2019. Highly microporous carbons from olive tree pruning: Optimization of chemical activation conditions. Journal of Environmental Chemical Engineering, 7 (1). https://doi.org/10.1016/j.jece.2018.102830

Md Arshad, S.H., Ngadi, N., Wong, S., Saidina, A.N., Razmi, F.A., Mohamed, N.B., Inuwa, I.M., Abdul Aziz, A., 2019. Optimization of phenol adsorption onto biochar from oil palm empty fruit bunch (EFB). Malaysian Journal of Fundamental and Applied Sciences, 15 (1), Pp. 1–5. https://doi.org/10.11113/mjfas.v15n2019.1199

Mopoung, S., Moonsri, P., Palas, W., Khumpai, S., 2015. Characterization and Properties of Activated Carbon Prepared from Tamarind Seeds by KOH Activation for Fe (III) Adsorption from Aqueous Solution. Scientific World Journal, 2015. https://doi.org/10.1155/2015/415961

Nedjai, R., Kabbashi, N.A., Alkhatib, M.F.R., Alam, M.Z., 2021. Removal of Phenol from Aqueous Solution by Adsorption onto Baobab Fruit Shell Activated Carbon: Equilibrium and Kinetics Studies. Journal of Environmental Treatment Techniques, 9 (3), Pp. 686–697.

Niasar, H.S., Li, H., Das, S., Kasanneni, T.V.R., Ray, M.B., Xu, C., 2018. Preparation of activated petroleum coke for removal of naphthenic acids model compounds: Box-Behnken design optimization of KOH activation process. Journal of Environmental Management, 211, Pp. 63–72. https://doi.org/10.1016/j.jenvman.2018.01.051

Ochando-Pulido, J.M., González-Hernández, R., Martinez-Ferez, A., 2018. On the effect of the operating parameters for two-phase olive-oil washing wastewater combined phenolic compounds recovery and reclamation by novel ion exchange resins. Separation and Purification Technology, 195, Pp. 50–59. https://doi.org/10.1016/j.seppur.2017.11.075

Ogando, F.I.B., Aguiar, C.L.D., Viotto, J.V.N., Heredia, F.J., Hernanz, D., 2019. Removal of phenolic, turbidity and color in sugarcane juice by electrocoagulation as a sulfur-free process. Food Research International, 122, Pp. 643–652. https://doi.org/10.1016/j.foodres.2019.01.039

Rashed, M.N., 2013. Adsorption Technique for the Removal of Organic Pollutants from Water and Wastewater. Organic Pollutants - Monitoring, Risk and Treatment, 7, Pp. 167-194. https://doi.org/10.5772/54048

Sharma, N.K., Philip, L., 2014. Effect of cyanide on phenolics and aromatic hydrocarbons biodegradation under anaerobic and anoxic conditions. Chemical Engineering Journal, 256, Pp. 255–267. https://doi.org/10.1016/j.cej.2014.06.070

Sotomayor, F.J., Cychosz, K.A., Thommes, M., 2018. Characterization of Micro/Mesoporous Materials by Physisorption: Concepts and Case Studies. Acc. Mater. Surf. Res, 3 (2), Pp. 34–50.

Sridhar, R., Ramanane, U.U., Rajasimman, M., 2018. ZnO nanoparticles –

Synthesis, characterization and its application for phenol removal from synthetic and pharmaceutical industry wastewater. Environmental Nanotechnology, Monitoring and Management, 10, Pp. 388–393. https://doi.org/10.1016/j.enmm.2018.09.003

Sudibandriyo, M., Kusumadewi, F., 2018. Hydrogen recovery from hydrogen-methane gas mixture using coffee grounds based activated carbon bioadsorbent. E3S Web of Conferences, 67, Pp. 1–6. https://doi.org/10.1051/e3sconf/20186702046

Sunil, K., Jayant, K., 2013. Adsorption for Phenol Removal-A Review. International Journal of Scientific Engineering and Research (IJSER), 1 (2), Pp. 2347–3878.

Víctor-Ortega, M.D., Ochando-Pulido, J.M., Martínez-Ferez, A., 2016. Performance and modeling of continuous ion exchange processes for phenols recovery from olive mill wastewater. Process Safety and Environmental Protection, 100, Pp. 242–251. https://doi.org/10.1016/j.psep.2016.01.017

Vunain, E., Biswick, T., 2018. Adsorptive removal of methylene blue from aqueous solution on activated carbon prepared from Malawian baobab fruit shell wastes: Equilibrium , kinetics and thermodynamic studies and thermodynamic studies. Separation Science and Technology, 54 (1), Pp. 27–41. https://doi.org/10.1080/01496395.2018.1504794

Vunain, E., Kenneth, D., Biswick, T., 2017. Synthesis and characterization of low-cost activated carbon prepared from Malawian baobab fruit shells by H3PO4 activation for removal of Cu (II) ions: equilibrium and kinetics studies. Applied Water Science, 7 (8), Pp. 4301–4319. https://doi.org/10.1007/s13201-017-0573-x

Xie, B., Qin, J., Wang, S., Li, X., Sun, H., Chen, W., 2020. Adsorption of Phenol on Commercial Activated Carbons: Modelling and Interpretation. International Journal of Environmental Research and Public Health, 17 (3), Pp. 789. https://doi.org/10.3390/ijerph17030789

Yahya, M.A., Al-Qodah, Z., Ngah, C.W.Z., 2015. Agricultural bio-waste materials as potential sustainable precursors used for activated carbon production: A review. Renewable and Sustainable Energy Reviews, 46, Pp. 218–235. https://doi.org/10.1016/j.rser.2015.02.051

Zagklis, D.P., Vavouraki, A.I., Kornaros, M.E., Paraskeva, C.A., 2015. Purification of olive mill wastewater phenols through membrane filtration and resin adsorption/desorption. Journal of Hazardous Materials, 285, Pp. 69–76. https://doi.org/10.1016/j.jhazmat.2014.11.038